In Situ Studies on the Irradiation-Induced Twin Boundary-Defect Interactions in Cu

C. FAN, JIN LI, ZHE FAN, H. WANG, and X. ZHANG

Polycrystalline Cu films with nanoscale annealing twins are subjected to *in situ* Kr^{++} ion irradiation at room temperature inside a transmission electron microscope up to a dose of 1 displacement-per-atom. Radiation induces prominent migration of incoherent twin boundaries. Depending on twin thickness, three types of twin boundary evolutions are observed, including rapid detwinning, gradual detwinning, and self-healing. The mechanism of twin thickness-dependent evolution of microstructures is discussed. This study provides further evidence on twin boundary-defect interactions and may assist the design of radiation-tolerant twinned metallic materials.

DOI: 10.1007/s11661-017-4293-5

I. INTRODUCTION

NANOTWINNED (nt) metals have raised significant attention due to their remarkable electrical conductivity,[1–3] thermal stability,[4,5] and excellent mechanical properties.[6–11] Prior studies show that twin thickness (t), the spacing between coherent twin boundaries (CTBs), plays a significant role in determining their physical and mechanical properties.[12–14] When twin thickness is reduced to a critical value, nanotwins may become unstable as shown by detwinning events occurring under high temperature,[15] electrical field,[16] and mechanical stress.[17] The detwinning behavior is directly correlated to the migration of partials on incoherent twin boundaries (ITBs).[18] According to the experimental studies using high-resolution transmission electron microscopy (HRTEM)[19–21] and atomistic simulations,[22,23] ITBs are composed of groups of Shockley partial dislocations on three successive {111} planes and tend to glide collectively under shear stress,[17,22–25] thereby causing detwinning.[26]

There are increasing investigations on radiation response of nt metals,[27–34] and radiation-induced detwinning has also been observed.[35] Li *et al.*[28] reported ITB migration in Cu film after Cu^{3+} ion irradiation, and attributed their migration to the glide of grain boundary Shockley partial dislocations, driven by concurrent reduction in radiation-induced defects. Yu *et al.*[30] observed continuous migration and recovery of ITB steps at the corners of thick twins in epitaxial nt Ag film under *in situ* Kr^{++} ion irradiation and inferred that the TB evolution is due to defect–ITB interactions. Song *et al.*[31] studied radiation-induced TB migration in Fe using atomistic simulations and demonstrated that the migration event might be enhanced by local thermal spikes and defect clusters. Chen *et al.*[35] reported that the radiation-induced detwinning in nt-Cu depends on twin thickness: the thinner the twins the faster the detwinning process. These studies suggest that radiation-induced detwinning is closely associated with the interaction between ITBs and radiation-induced defect clusters.

In this paper, we examined the radiation-induced detwinning for twins of various thicknesses in annealed Cu subjected to *in situ* Kr^{++} ion irradiation experiment. Several distinct types of defect–ITB interactions were identified. The underlying mechanisms of radiation-induced thickness-dependent detwinning are compared. This study contributes to the further understanding on heavy ion irradiation response of nt metals.

II. EXPERIMENTAL

Cu films, ~80 nm in thickness, were DC sputter deposited at room temperature using 99.99 pct purity Cu target onto sample grids supported with carbon film for transmission electron microscopy (TEM) studies. Prior to deposition, the chamber was evacuated to a

C. FAN and X. ZHANG are with the School of Materials Engineering, Purdue University, West Lafayette, IN 47907. Contact e-mail: xzhang98@purdue.edu JIN LI is with the School of Materials Engineering, Purdue University, and also with the Department of Materials Science and Engineering, Texas A&M University, College Station, TX 77843-3123. ZHE FAN is with the School of Materials Engineering, Purdue University, and also with the Department of Mechanical Engineering, Texas A&M University, College Station, TX 77843-3123. H. WANG is with the School of Materials Engineering, Purdue University, and also with the School of Electrical and Computer Engineering, Purdue University, West Lafayette, IN 47907.
Manuscript submitted May 20, 2017.
Article published online August 23, 2017

base pressure of ~8 × 10^{-8} torr. Isothermal annealing was then performed for 20 minutes at 573 K (300 °C) in ultra-high purity Argon gas. After annealing, a large number of annealing twins with various thicknesses were introduced in large grains. *In situ* Kr^{++} ion radiation was conducted at room temperature at the Intermediate Voltage Electron Microscopy (IVEM) facility at Argonne National Laboratory. 1 MeV Kr^{++} ion beam was utilized for the radiation experiment, during which a CCD camera was used to capture microstructural evolution at 15 frames/s. Radiation damage in terms of displacement-per-atom (dpa) inside Cu film was calculated using the SRIM (Stopping and Range of Ions in Matter) simulation with the Kinch–Pease method.[36,37] The average dose rate was controlled at 2.5 × 10^{-3} dpa/s. The temperature rise of the sample during irradiation was measured to be less than 283 K (10 °C)

III. RESULTS

A. *Radiation-Induced Detwinning*

To explore the detailed morphology evolution process, large Cu grains with numerous annealing twins of various thickness were selected for examinations. Figure 1(a) shows a typical example where 7 well-defined twins (labeled by arrows) in a Cu grain were monitored during their irradiations. All of these twins have one of their ITBs terminated in grain interior, and they are oriented in two sets of {111} planes at an interception angle of 71 deg. Figures 1(b) through (d) show morphology evolutions for several twins up to 1 dpa. Several ultrafine twins 1, 2, and 7 with thickness $t < 10$ nm, underwent drastic ITB migration and completely detwinned (after irradiation in Figure 1(d)). Meanwhile, twins 4 and 5 with intermedium thickness ($10 < t < 20$ nm) experienced incomplete detwinning, shortened from their original lengths of 203 and 108 to 168 and 82 nm (see Figure 1(d)), respectively. However, thicker twins, 3 and 6 ($t > 20$ nm), survived the heavy ion irradiation with little ITB migration. The detwinning events are summarized and schematically illustrated in Figure 1(e), where the areas arising from ITB migrations are outlined by dashed lines. It is worth noting that no significant CTB migrations were observed, and the twins with both ends of ITBs anchored at the grain boundaries remained stable after irradiation.

In situ TEM studies enable us to track the ITB migration processes in real time. The reduction of twin length shown in Figure 2(a) is a direct consequence of radiation-induced detwinning. Furthermore thinner twins have higher ITB migration velocity (V_{ITB}) as shown by the red circles in Figure 2(b), which is consistent with the data (shown as blue squares) derived from our previous studies on radiation-induced detwinning in epitaxial nt-Cu films.[35] Moreover, radiation-induced detwinning also depends on dose rate. The dose rate in the current study is $K_1 = 2.5 \times 10^{-3}$ dpa/s, higher than our previous study, $K_2 = 0.43$ to 1.98 × 10^{-3} dpa/s.[35] A comparison of these two sets of studies reveals that V_{ITB} increases with increasing dose rate for the twins that are less than 20 nm in thickness. However, when the twins are thicker than 20 nm, there are little ITB migration. In fact, ITBs tend to migrate at room temperature even without irradiation, which is driven by the excess energy stored in CTBs. Atomistic simulations have revealed that when the twin thickness is less than 2 nm, the driving force becomes so large that detwinning process can easily occur (in Cu) at room temperature (without irradiation).[18] The value of V_{ITB} of the non-irradiation case can be calculated based on annealing experiment,[15] and it is also plotted as a black reference line in Figure 2(b). At room temperature, TBs in Cu barely migrate unless they are extremely fine. In contrast, radiation has prominently accelerated detwinning velocity for twins of various thickness.

B. *Defect–ITB Interactions and Morphology Evolutions*

Heavy ion irradiation induces a large number of defect clusters in annealed Cu, and Figure 3 shows the statistics on the distributions of size (D) and lifetime (T) of defects. The defects have an average diameter (D_{avg}) of 4.4 nm and an average lifetime (T_{avg}) of 15.0 seconds.

In addition, frequent defect–ITB interactions were observed by carefully examining the *in situ* TEM videos. Figure 4 shows two distinct types of defect–ITB interactions for a twin T4, consisting of an ultrafine tip $T4^a$ with a thickness t_4^a of 8 nm, and a medium-thick twin base $T4^b$ with a thickness t_4^b of 17 nm. The defect–ITB interactions led to the removal of $T4^a$ through two steps: a sharpening process as shown in Figures 4(a) through (c), and a collapse process as shown in Figures 4(d) through (f). At 78 seconds in Figure 4(a), $T4^a$ had a flat end and a dislocation loop L1 was formed in its vicinity. At 80 seconds in Figure 4(b), L1 began to grow and approached $T4^a$, and a direct contact (DC) occurred afterwards. At 94 seconds in Figure 4(c), L1 was entirely absorbed and $T4^a$ became pointed. The tip remained sharp for ~46 seconds, see Figure 4(d). However, once L2 emerged near $T4^a$ at 139.13 seconds in Figure 4(e), the sharp $T4^a$ collapsed as evidenced by instant detwinning at 139.40 seconds in Figure 4(f); in other words, a non-contact (NC) defect-TB interaction had occurred. The detwinning velocity is ~80 nm/s. More details related to the DC and NC interactions can be found in Supplementary Video SV1 and SV2, respectively.

In addition to the drastic detwinning at the tip of the ultrafine twin T4, a gradual detwinning event was observed. Figures 5(a) through (c) demonstrate the morphology evolution of twin T1 ($t_1 = 10$ nm) with increasing dose. At 50 seconds in Figure 5(a), T1 was 60 nm long. During irradiation, it was shortened to 41 nm in 30 seconds (Figure 5(b)), and then shrank to 18 nm in length at 370 seconds as shown in Figure 5(c). Meanwhile, frequent defect–ITB interactions were also captured, and two typical defect clusters that interacted with ITB are marked as L3 and L4. The average detwinning velocity for T1 is calculated to be ~0.12 nm/

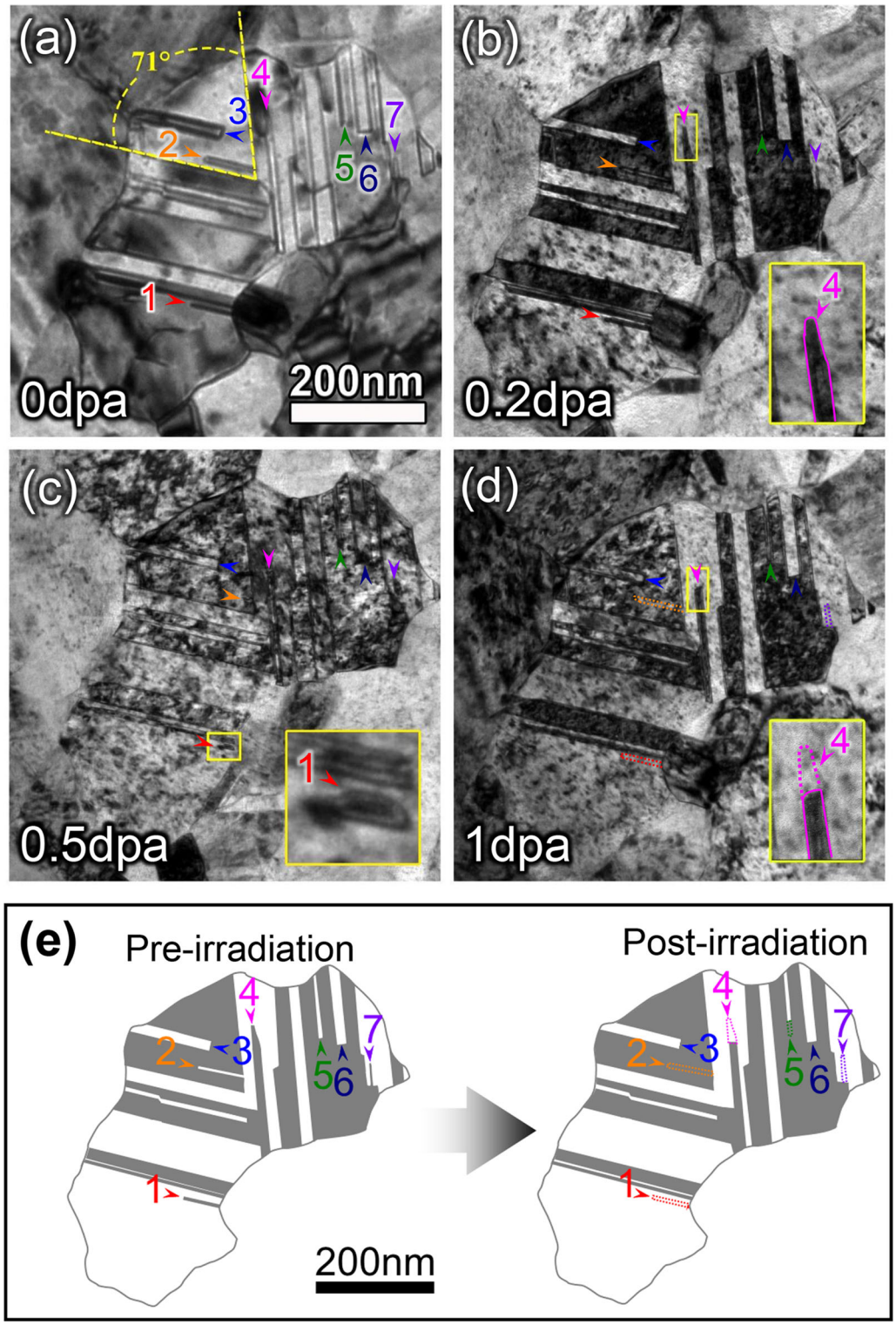

Fig. 1—*In situ* TEM snapshots and schematic illustration showing detwinning for various annealing twins inside a large Cu grain subjected to Kr^{++} ion irradiation up to 1 dpa at room temperature. (*a* through *d*) Sequential TEM micrographs taken at different doses showing the morphology evolution of several twins labeled as 1 to 7. The insets in (*b*) and (d) show the enlarged images of the end of twin 4, and the inset in (*c*) shows the remaining section of twin 1 at 0.5 dpa. (*e*) Schematic illustration depicting the morphology variation of the labeled twins (Color figure online).

s. In comparison, a thick twin T6 ($t_6 = 25$ nm) showed self-healing capability. As shown in Figure 5(d), the corners of T6 were very sharp at 50 seconds, but they became blunted at 86 seconds (Figure 5(e)). By 156 seconds as shown in Figure 5(f), the two blunted corners became sharp (orthogonal) again. More details related

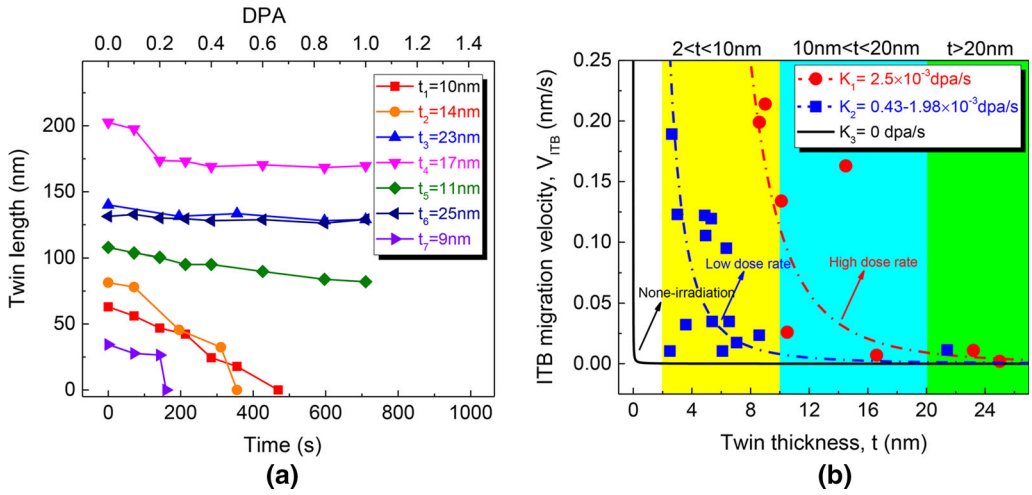

Fig. 2—The dependence of ITB migration on twin thickness and dose rate at room temperature. (*a*) The plot of twin length over radiation dose for numerous twins. (*b*) The average ITB migration velocity (V_{ITB}) of the current study (plotted in red) decreases rapidly with increasing twin thickness at a high dose rate of $K_1 = 2.5 \times 10^{-3}$ dpa/s. The reference data of a low dose rate[35] ($K_1 = 0.41$ to 1.98×10^{-3} dpa/s) and non-irradiation[15] ($K_3 = 0$ dpa/s) are also plotted in blue and black, respectively (Color figure online).

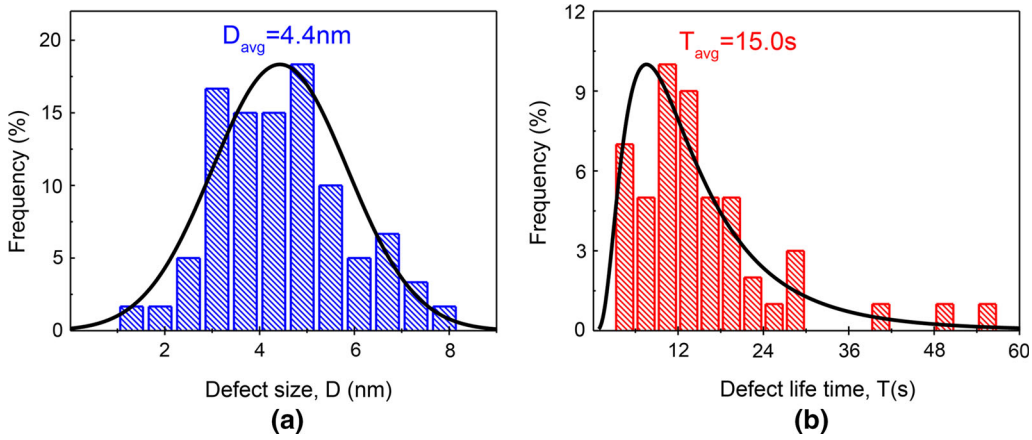

Fig. 3—Histograms showing the statistics of (*a*) diameter D and (*b*) lifetime T of radiation-induced defect clusters in twinned Cu. The average defect size (D_{avg}) and lifetime (T_{avg}) are measured to be 5 nm and 15.0 s, respectively.

to the gradual detwinning of T1 and the self-healing capacity of T6 can be found in Supplementary Video SV3 (accelerated by 5 times) and SV4 (accelerated by 5 times), respectively.

IV. DISCUSSION

A. *Irradiation-induced Detwinning*

To understand the detwinning behavior under irradiation, it is necessary to examine the ITB microstructure and its migration mechanism. Most twinning or detwinning processes typically occur *via* collective glide of multiple twin dislocations (TDs) in ITBs.[18,23,24] In face-centered cubic (FCC) metals, ITBs are composed of a set of three Shockley partial dislocations $1/6\langle 112\rangle$ on adjacent $\{111\}$ planes.[22] These partials can migrate under applied shear stress, resulting in ITB migration[17,25,38] with a velocity V that can be expressed as[15]:

$$V = \frac{2\gamma}{t} M_0 e^{\left(-\frac{\Delta Q}{kT}\right)}, \qquad [1]$$

where t is the twin thickness, ΔQ is activation energy, k is Boltzmann's constant, and T is temperature. $M_0 e^{\left(-\frac{\Delta Q}{kT}\right)}$ is defined as the ITB migration mobility, and $\frac{2\gamma}{t}$ is the net pressure or the main driving force of detwinning arising from the excess CTB energy γ, about 24 mJ/m^2 for Cu.[39]

For the case of non-irradiation detwinning at room temperature as shown in Figure 2(b), its activation energy has been measured as ~0.90 eV/atom.[15] Under irradiation, ITB migration velocity accelerates significantly, especially for the twins thinner than 20 nm. Using Eq. [1], we can determine that the average

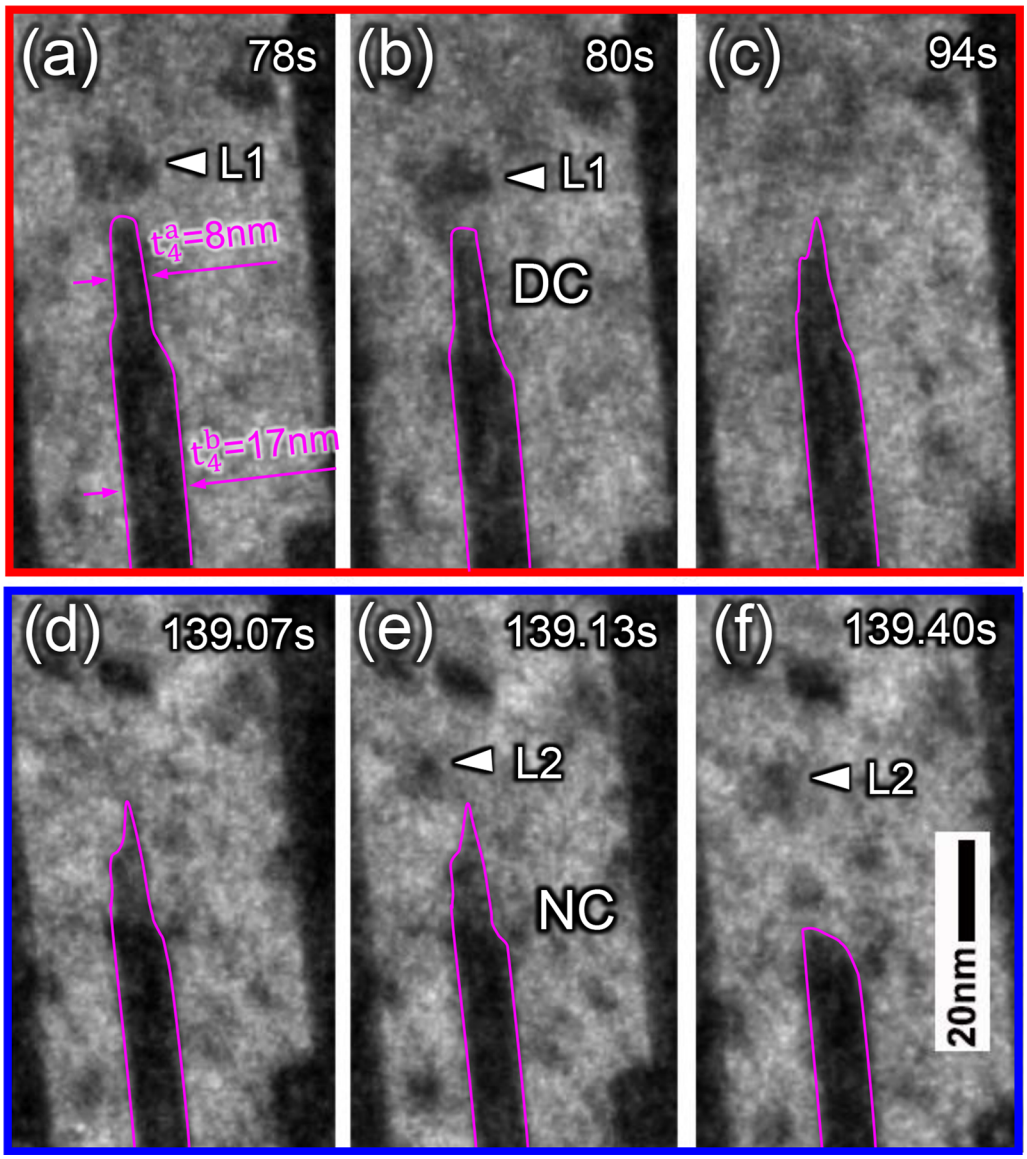

Fig.4—A series of TEM snapshots taken during *in situ* irradiation of nt-Cu over 0.1 to 0.2 dpa, showing the detwinning process for twin T4. Its tip section $T4^a$ has a thickness of 8 nm, whereas the base portion, $T4^b$, is 17 nm thick. Two radiation-induced dislocation loops interacting with the ITB are indicated by L1 and L2. (*a* through *c*) The sharpening process of $T4^a$ caused by its direct contact (DC) with L1. (*d* through *f*) The subsequent collapse of $T4^a$ triggered by its non-contact (NC) interaction with L2. See Supplementary Videos of SV1 and SV2 for more details.

activation energy for the current irradiation-induced TB migration is much lower, ~0.42 eV/atom. The reduced activation energy is attributed to the local shear stress τ arising from radiation-induced defect clusters.[31] According to the defect reaction rate theory,[40] ΔQ can be expressed in terms of shear stress τ as:

$$\Delta Q = \Delta Q_0 \left(1 - \frac{\tau}{\tau^c}\right)^{\alpha}, \qquad [2]$$

where ΔQ_0 is the activation energy at $\tau = 0$, and τ^c is the critical stress and α is a dimensionless exponential factor. MD simulations have revealed that the activation energy barrier and critical activation stress can be lowered in the existence of irradiation-induced defect clusters.[31] Under heavy ion irradiation, numerous defect clusters are generated, and they can continuously impinge ITBs (see Figure 4) and apply shear stress on Shockley partials along ITBs. Consequently, the activation energy is reduced and the ITB migration velocity increases.

B. *Defect–ITB Interactions*

Figure 4 shows two distinct types of defect–ITB interactions that are defined as DC and NC. On the one hand, DC occurs when a defect cluster is in direct contact with an ITB and is subsequently absorbed by the ITB. In FCC metals, heavy ion irradiation generates point defect clusters in the form of dislocation loops, stacking fault tetrahedron (SFT), and voids.[41–43] Among them, dislocation loops are the most commonly observed, including both faulted and perfect loops.[44–48] The perfect dislocation loops are glissile and able to diffuse very fast in the closely packed ⟨110⟩ direction

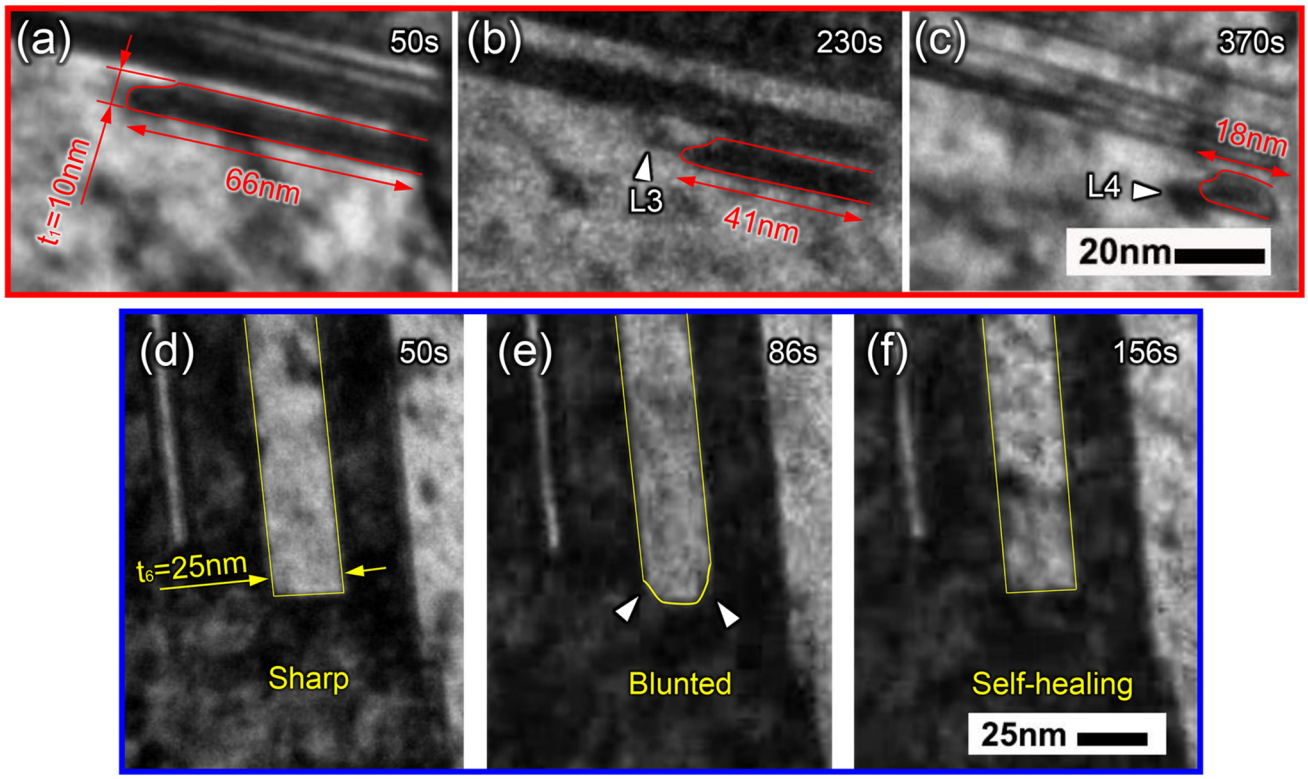

Fig.5—*In situ* TEM observations showing the gradual detwinning of twin T1 and the self-healing capability of twin T6. (*a* through *c*) The length of twin T1 (thickness t_1 = 10 nm) decreased from 66 to 41 nm by 230 s, and to 18 nm by 370 s. Meanwhile, two typical defect clusters that interacted with the ITB were captured, marked as L3 and L4. (*d* through *f*) Twin T6 (t_6 = 25 nm) had two sharp corners at 50 s, and by 86 s both corners became blunted. By 156 s, the TBs with blunted corners have recovered, exhibiting a self-healing ability. See Supplementary Videos of SV3 and SV4 for more details.

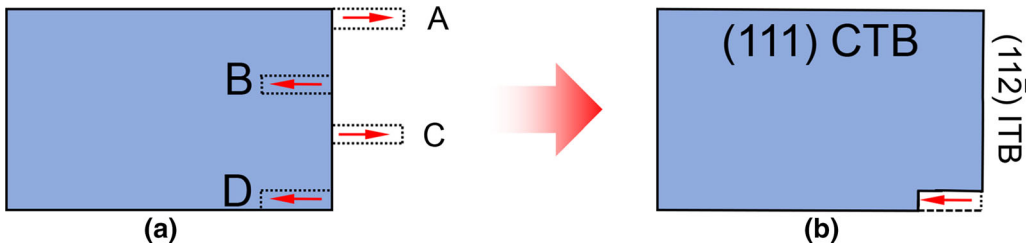

Fig. 6—Schematics illustrating how a thick twin engages defect clusters (not shown here) and starts its detwinning from the corner. (*a*) Four potential scenarios of ITB migration are presented, including A—corner twinning, B—middle detwinning, C—middle twinning, and D—corner detwinning. (*b*) The corner detwinning of scenario D is more energetically favorable than the others, and it occurs more frequently in experiment.

along their Burgers vector.[49–51] The mobility of perfect dislocation loops inevitably facilitates their interactions with ITBs, which may lead to the formation of Frank partials by:

$$\frac{1}{2}[\bar{1}\bar{1}0]+\frac{1}{6}[112]\rightarrow\frac{1}{3}[\bar{1}\bar{1}1]. \qquad [3]$$

The Frank partials formed in ITBs are sessile and cannot glide under shear stress, but they may migrate back and forth *via* dislocation climb by absorbing vacancies or interstitials. This mechanism can partially explain the ITB's sharpening process observed in Figures 4(a) through (c) and its self-healing capacity as shown in Figures 5(d) through (f). On the other hand, these Frank partials can further absorb perfect loops with the opposite Burgers vector, resulting in their reverse transformation into Shockley partials through the following reaction:

$$\frac{1}{2}[110]+\frac{1}{3}[\bar{1}\bar{1}1]\rightarrow\frac{1}{6}[112]. \qquad [4]$$

When ITBs are decorated by Shockley partials, they become mobile again and can migrate rapidly through stress-driven dislocation glide. NC can now occur through the mechanical impingement of adjoining defects on ITBs, as shown in Figures 4(d) through (f).

In addition, it is worth pointing out that the characteristic of defect size and lifetime plays an important role in defect–ITB interactions. Statistic studies in Figure 3 show that the dimension of defect clusters is smaller

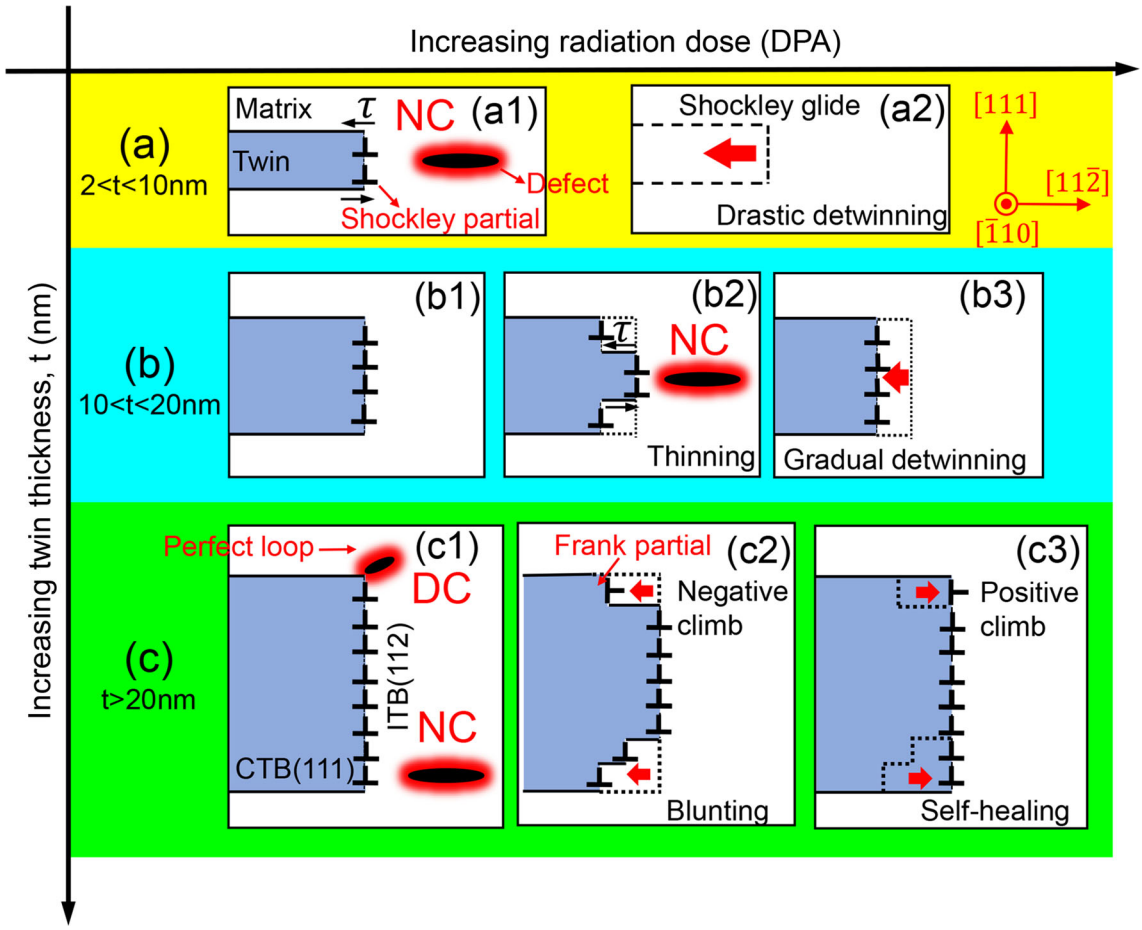

Fig.7—Schematic illustration of twin thickness-dependent detwinning during radiation. Two types of defect–ITB interactions, direct contact (DC) and non-contact (NC) interactions are marked. (*a1*), (*a2*) The drastic detwinning of ultrathin twins ($t < 10$ nm) occurs *via* the glide of Shockley partials on ITBs. (*b1*), (*b3*) The gradual detwinning of medium-thick twins ($10 < t < 20$ nm), which starts from corner (sharping or thinning of the twin) and subsequent collapses of the sharpened tip. (*c1* through *c3*) The self-healing capacity of thick twins ($t > 20$ nm) occurs through negative or positive Frank climb at corners along thick ITBs or glide of Shockley partials from their ITB corners.

than 10 nm and their lifetime is shorter than 60 seconds. This observation leads us to hypothesize that the influence of a defect cluster on an ITB may be limited by both space and time scale. For a thick twin, larger than 20 nm in thickness, there would be 4 representative scenarios of defect–ITB interactions, shown schematically in Figure 6(a), including A—corner twinning, B—middle detwinning, C—middle twinning, and D—corner detwinning. Here twinning (detwinning) refers to the extension (contraction) of an existing twin. Note that the first three scenarios, A, B, and C, lead to the increase of the length of CTBs. Considering the small size and short lifetime of defect clusters, the scenarios of A, B, and C are less energetically favorable than the scenario D in Figure 6(a). Consequently, the defect–ITB interactions for a thick twin may lead to detwinning process from the corner, as shown in Figure 6(b).

C. *Thickness-Dependent Detwinning*

We finally discuss the thickness-dependent detwinning mechanism for twinned Cu under Kr^{++} irradiation. The mechanism is schematically illustrated in Figure 7 and summarized as follows:

(1) The ultrathin twins ($t < 10$ nm) in Figures 7(a1), (a2), with a thickness comparable to the size of radiation-induced defect clusters, may be more likely to undergo drastic detwinning *via* the glide of Shockley partials on ITBs. The drastic detwinning event may be triggered by local shear stress (τ) arising from a dislocation loop that is not in direct contact with the ITB (NC mode).

(2) The twins with medium thickness ($10 < t < 20$ nm) shown in Figures 7(b1) through (b3) may first experience a thinning process at twin corners. Then the sharpened tip may go through a rapid collapsing process resulting in a gradual detwinning.

(3) The thick twins ($t > 20$ nm) shown in Figures 7(c1), (c2), are only subject to detwinning at twin corners through DC or NC interactions. After DC interactions, Frank partials are formed in ITBs, which are immobile and can slow down the detwinning process significantly. Meanwhile,

Frank partials can have positive or negative climb by absorbing vacancies or interstitials, and Shockley partials can glide back and forth in accordance with the direction of local shear stress. As a result, thick twins can recover from their blunted outlines and possess a self-healing capacity.

The aforementioned detwinning mechanism is concluded based on defect–ITB interactions, which implies that the defect density around an ITB plays an important role in its migration. There are two factors that can influence the defect density. First, increasing dose rate can induce more defects, accompanied with more frequent defect–ITB interactions and faster ITB migration velocity as shown in Figure 2(b). Second, TBs and grain boundaries (GBs) can act as effective trapping sites that can influence defect formation and distribution.[52–54] For instance, T1, T7, and T5 have similar twin thicknesses, ~10 nm, but they have different length reductions after irradiation. Note that T5 is sandwiched between two TBs, but only one side of T1 and T7 has a TB. It can be inferred that less defects were formed in the matrix around T5, causing less detwinning, while more defects interacted with T1 and T7, leading to their full detwinning. In addition, thinner twins of T1, T2, and T7 in Figure 2(a) became rather unstable when their lengths were shortened down to 25 nm. As they became shorter, their ITBs migrated rapidly towards the GBs. Twin T5 had an original length over 100 nm, and it detwinned much less than the shorter twins (T1 and T7 with a length of ~63 and 35 nm, respectively) did under the same irradiation condition.

V. CONCLUSION

Using *in situ* Kr^{++} ion irradiation, we have studied the radiation-induced detwinning in Cu containing high-density annealing twins. The detwinning event exhibits dose rate-dependence and thickness-dependence. Higher dose rate accelerates detwinning. Moreover, for thinner twins, less than 20 nm in thickness, radiation significantly accelerates the TB migration velocity. However, when the twin thickness exceeds a critical value, ~20 nm in the current study, twins tend to show self-healing capability as evidenced by back-and-forth migration of ITBs from corners. Two types of defect–ITB interaction modes, direct and non-direct contact, have been observed and account for the thickness-dependent detwinning mechanism.

ACKNOWLEDGMENTS

We acknowledge financial support by NSF-DMR-Metallic Materials and Nanostructures Program under Grant No. 1643915. H.W. acknowledges the support from the U.S. Office of Naval Research (N00014-16-1-2778). The work on the fabrication of nanotwinned metals is supported by DOE-OBES under Grant No. DE-SC0016337. We also thank Peter M. Baldo and Edward A. Ryan at Argonne National Laboratory for their help during *in situ* radiation experiments. The IVEM facility at Argonne National Laboratory is supported by DOE-Office of Nuclear Energy. Access to the Microscopy Center at Purdue University is also acknowledged.

ELECTRONIC SUPPLEMENTARY MATERIAL

The online version of this article (doi: 10.1007/s11661-017-4293-5) contains supplementary material, which is available to authorized users.

REFERENCES

1. X.H. Chen, L. Lu, and K. Lu: *J. Appl. Phys.*, 2007, vol. 102, p. 083708.
2. L. Lei, Y. Shen, X. Chen, L. Qian, and L. Ke: *Science*, 2004, vol. 304, pp. 422–26.
3. O. Anderoglu, A. Misra, H. Wang, F. Ronning, M.F. Hundley, and X. Zhang: *J. Appl. Phys.*, 2008, vol. 93, p. 083108.
4. O. Anderoglu, A. Misra, H. Wang, and X. Zhang: *J. Appl. Phys.*, 2008, vol. 103, p. 094322.
5. X. Zhang, A. Misra, H. Wang, J.G. Swadener, A.L. Lima, M.F. Hundley, and R.G. Hoagland: *Appl. Phys. Lett.*, 2005, vol. 87, p. 233116.
6. X. Zhang, A. Misra, H. Wang, T.D. Shen, M. Nastasi, T.E. Mitchell, J.P. Hirth, R.G. Hoagland, and J.D. Embury: *Acta Mater.*, 2004, vol. 52, pp. 995–1002.
7. M. Dao, L. Lu, Y.F. Shen, and S. Suresh: *Acta Mater.*, 2006, vol. 54, pp. 5421–32.
8. L. Ke, L. Lu, and S. Suresh: *Science*, 2009, vol. 324, pp. 349–52.
9. F. Sansoz, K. Lu, T. Zhu, and A. Misra: *MRS Bull.*, 2016, vol. 41, pp. 292–97.
10. J. Wang and X. Zhang: *MRS Bull.*, 2016, vol. 41, pp. 274–81.
11. D. Bufford, H. Wang, and X. Zhang: *Acta Mater.*, 2011, vol. 59, pp. 93–101.
12. L. Lu, X. Chen, X. Huang, and K. Lu: *Science*, 2009, vol. 323, pp. 607–10.
13. X. Li, Y. Wei, L. Lei, L. Ke, and H. Gao: *Nature*, 2010, vol. 464, pp. 877–80.
14. I.J. Beyerlein, X. Zhang, and A. Misra: *Annu. Rev. Mater. Res.*, 2014, vol. 44, pp. 329–63.
15. J. Miao: *J. Appl. Phys.*, 2008, vol. 104, p. 113717.
16. K.-C. Chen, W. Wen-Wei, C.-N. Liao, L.-J. Chen, and K.N. Tu: *J. Appl. Phys.*, 2010, vol. 108, p. 066103.
17. Y. Liu, J. Jian, Y. Chen, H. Wang, and X. Zhang: *Appl. Phys. Lett.*, 2014, vol. 104, p. 231910.
18. J. Wang, N. Li, O. Anderoglu, X. Zhang, A. Misra, J.Y. Huang, and J.P. Hirth: *Acta Mater.*, 2010, vol. 58, pp. 2262–70.
19. G.H. Campbell, D.K. Chan, D.L. Medlin, J.E. Angelo, and C.B. Carter: *Scripta Mater.*, 1996, vol. 35, pp. 837–42.
20. C.B. Carter, D.L. Medlin, J.E. Angelo, and M.J. Mills: *Mater. Sci. Forum*, 1996, vol. 27, pp. 209–12.
21. D.L. Medlin, G.H. Campbell, and C.B. Carter: *Acta Mater.*, 1998, vol. 46, pp. 5135–42.
22. J. Wang, O. Anderoglu, J.P. Hirth, A. Misra, and X. Zhang: *Appl. Phys. Lett*, 2009, vol. 95, p. 021908.
23. J. Wang, A. Misra, and J.P. Hirth: *Phys. Rev. B*, 2011, vol. 83, p. 064106.
24. G. Van Tendeloo, D. Broddin, H.W. Zandbergen, and S. Amelinckx: *Phys. C*, 1990, vol. 167, pp. 627–39.
25. N. Li, J. Wang, J.Y. Huang, A. Misra, and X. Zhang: *Scripta Mater.*, 2011, vol. 64, pp. 149–52.
26. A.M. Hodge, T.A. Furnish, C.J. Shute, Y. Liao, X. Huang, C.S. Hong, Y.T. Zhu, T.W. Barbee, Jr, and J.R. Weertman: *Scripta Mater.*, 2012, vol. 66, pp. 872–77.

27. M.J. Demkowicz, O. Anderoglu, X. Zhang, and A. Misra: *J. Mater. Res.*, 2011, vol. 26, pp. 1666–75.
28. N. Li, J. Wang, Y.Q. Wang, Y. Serruys, M. Nastasi, and A. Misra: *J. Appl. Phys.*, 2013, vol. 113, p. 023508.
29. K.Y. Yu, D. Bufford, C. Sun, Y. Liu, H. Wang, M.A. Kirk, M. Li, and X. Zhang: *Nat. Commun.*, 2013, vol. 4, p. 1377.
30. K.Y. Yu, D. Bufford, F. Khatkhatay, H. Wang, M.A. Kirk, and X. Zhang: *Scripta Mater.*, 2013, vol. 69, p. 385.
31. D. Song, X. Li, J. Xue, H. Duan, and Z. Jin: *Philos. Mag. Lett.*, 2014, vol. 94, pp. 361–69.
32. Y. Chen, K.Y. Yu, Y. Liu, S. Shao, H. Wang, M.A. Kirk, J. Wang, and X. Zhang: *Nat. Commun.*, 2015, vol. 6, p. 7036.
33. J. Li, K.Y. Yu, Y. Chen, M. Song, H. Wang, M.A. Kirk, M. Li, and X. Zhang: *Nano Lett.*, 2015, vol. 15, pp. 2922–27.
34. Y. Chen, J. Li, K.Y. Yu, H. Wang, M.A. Kirk, M. Li, and X. Zhang: *Acta Mater.*, 2016, vol. 111, pp. 148–56.
35. Y. Chen, H. Wang, M.A. Kirk, M. Li, J. Wang, and X. Zhang: *Scripta Mater.*, 2017, vol. 130, pp. 37–41.
36. J.F. Ziegler, M.D. Ziegler, and J.P. Biersack: *Nucl. Instrum. Methods Phys. Res., Sect. B*, 2010, vol. 268, pp. 1818–23.
37. R.E. Stoller, M.B. Toloczko, G.S. Was, A.G. Certain, S. Dwaraknath, and F.A. Garner: *Nucl. Instrum. Methods Phys. Res., Sect. B*, 2013, vol. 310, pp. 75–80.
38. N. Li, J. Wang, A. Misra, X. Zhang, J.Y. Huang, and J.P. Hirth: *Acta Mater.*, 2011, vol. 59, pp. 5989–96.
39. D. Xu, W.L. Kwan, K. Chen, X. Zhang, V. Ozoliņš, and K.N. Tu: *Appl. Phys. Lett.*, 2007, vol. 91, p. 254105.
40. T. Zhu, J. Li, A. Samanta, A. Leach, and K. Gall: *Phys. Rev. Lett.*, 2008, vol. 100, p. 025502.
41. S.J. Zinkle: *Compr. Nucl. Mater.*, 2012, vol. 1, pp. 65–98.
42. D. Brian: Wirth*Science*, 2007, vol. 318, pp. 923–24.
43. S.J. Zinkle and K. Farrell: *J. Nucl. Mater.*, 1989, vol. 168, pp. 262–67.
44. Y. Osetsky, D.J. Bacon, A. Serra, B.N. Singh, and S.I. Golubov: *J. Nucl. Mater.*, 2000, vol. 276, pp. 65–77.
45. D.J. Bacon, Y.N. Osetsky, R. Stoller, and R.E. Voskoboinikov: *J. Nucl. Mater.*, 2003, vol. 323, pp. 152–62.
46. M.L. Jenkins: *Philos. Mag.*, 1974, vol. 29, pp. 813–28.
47. M.L. Jenkins, D.J.H. Cockayne, and M.J. Whelan: *J. Microsc.*, 1973, vol. 98, pp. 155–64.
48. M.L. Jenkins: *J. Nucl. Mater.*, 1994, vol. 216, pp. 124–56.
49. H. Abe, N. Sekimura, and Y. Yang: *J. Nucl. Mater.*, 2003, vol. 323, pp. 220–28.
50. Y. Matsukawa and S.J. Zinkle: *Science*, 2007, vol. 318, pp. 959–62.
51. K. Arakawa, K. Ono, H. Mori, A.S. Avilov, S.L. Dudarev and L.D. Marks, *AIP Conf. Proc.*, vol. 99, pp. 66–78.
52. X.-M. Bai, A.F. Voter, R.G. Hoagland, M. Nastasi, and B.P. Uberuaga: *Science*, 2010, vol. 327, pp. 1631–34.
53. J. Li, Y. Chen, H. Wang, and X. Zhang: *Metall. Mater. Trans. A*, 2017, vol. 48, pp. 1466–73.
54. M.K. Miller, C.M. Parish, and H. Bei: *J. Nucl. Mater.*, 2015, vol. 462, pp. 422–27.